Journal of Quantitative Spectroscopy & Radiative Transfer 229 (2019) 17–22

Contents lists available at ScienceDirect

Journal of Quantitative Spectroscopy & Radiative Transfer

journal homepage: www.elsevier.com/locate/jqsrt

Line positions and N_2-induced line parameters of the 00°3–00°0 band of $^{14}N_2{}^{16}O$ by comb-assisted cavity ring-down spectroscopy

G.-L. Liu[a], J. Wang[a,b], Y. Tan[a,b], P. Kang[a], Z. Bi[c], A.-W. Liu[a,b,*], S.-M. Hu[a]

[a] Hefei National Laboratory for Physical Sciences at Microscale, University of Science and Technology of China, Hefei 230026, China
[b] CAS Center for Excellence in Quantum Information and Quantum Physics, University of Science and Technology of China, Hefei 230026, China
[c] National Institute of Metrology, Beijing 100013, China

ARTICLE INFO

Article history:
Received 9 November 2018
Revised 28 January 2019
Accepted 6 March 2019
Available online 7 March 2019

Keywords:
Frequency comb
Cavity ring-down spectroscopy
Line position
Nitrous oxide
N_2-induced line parameters

ABSTRACT

Ro-vibrational transitions of the 00°3–00°0 band around 1.52 μm with line intensities in the order of 10^{-24} to 10^{-23} $cm^{-1}/(molecule{\cdot}cm^{-2})$ have been recorded using a comb-assisted laser-locked cavity ring-down spectrometer with high sensitivity as well as high precision. In total, 88 line positions were determined with a sub-MHz uncertainty (1-σ), better than previous experimental results by 1–2 order of magnitude. N_2-induced line shape parameters of 20 isolated transitions were derived by using the Voigt profile and the quadratic Speed-Dependent Voigt profile with relative uncertainties of 1–2% (1-σ). Comparisons of the line parameters determined in this work with literature experimental values are given.

1. Introduction

Nitrous oxide (N_2O) is an important trace constituent in the Earth's atmosphere as one of the major greenhouse gases in the troposphere, with a global warming potential of about 300 times greater than that of CO_2 [1,2]. Its contribution to the "dry" global greenhouse effect amounts to 6% as the Intergovernmental Panel on Climate Change (IPCC) claims [3]. Major efforts contribute the establishment of the network for the Total Carbon Column Observing Network (TCCON) [4,5], which use ground-based Fourier-transform infrared (FTIR) spectrometers distributed all over the world to measure atmospheric absorption spectra with solar radiation. It has been used to monitor the total column concentrations of the major greenhouse components in Earth's atmosphere. Accurate laboratory spectroscopic studies of its absorption line shapes in different spectral ranges are needed to enable satellite-based, ground-based, and airborne remote sensing measurements of N_2O. The knowledge of the line parameters is essential for atmospheric retrievals and it has been shown for various molecules that non-Voigt effects like line mixing or speed dependence of broadening have to be accounted for in atmospheric retrievals [6,7].

Highly accurate line positions of N_2O have been obtained by various methods. The results recently reported by Ting et al. in sub-Doppler regime have supplanted most of the previous studies in terms of accuracy of rotational transitions in N_2O [8]. The R(7) line around 1.28 μm has been measured with the noise-immune cavity-enhanced optical heterodyne molecular spectroscopy (NICE-OHMS) technique [9]. Al Saif et al. measured frequencies of 72 lines in the ν_1 fundamental band of $^{14}N_2{}^{16}O$ using a novel spectrometer that relies on locking an external-cavity quantum cascade laser around 7.8 μm to a Tm: based frequency comb at 1.9 μm [10]. Line parameters and the temperature dependences for the corresponding line-broadening coefficients have been derived from the Fourier-transform spectroscopy of nitrous oxide broadened by N_2, O_2, and N_2O in the 4 μm and 8 μm spectral regions [11]. There are also reports for N_2- and air-broadened line-widths and frequency-shifts for spectral lines in the range of 1800 - 4800 cm^{-1} [11], self-broadened line widths and pressure-induced line shifts of N_2O in the 1800–2630 cm^{-1} region [12], and also N_2- and O_2-broadened half-widths and their temperature dependences between 216 and 296 K for lines in the 4.5 μm region corresponding to the ν_3 fundamental band [13]. Vitcu et al. investigated the 0310 - 0110 parallel Q-branch of N_2O at 297 K in the pressure range of 11–30 Torr and determined self-broadened, pressure-induced shifts, and line-mixing coefficients [13]. Loos et al. reported highly accurate measurements of air-broadening, pressure-shift, speed dependence, and Rosenkranz line-mixing parameters for transitions in the ν_3 fundamental band of N_2O [2]. Recently, the 00°2 – 00°0

* Corresponding author.
E-mail addresses: lgl@mail.ustc.edu.cn (G.-L. Liu), jinwang@ustc.edu.cn (J. Wang), tanyan@ustc.edu.cn (Y. Tan), kpeng@mail.ustc.edu.cn (P. Kang), bizh@nim.ac.cn (Z. Bi), awliu@ustc.edu.cn (A.-W. Liu), smhu@ustc.edu.cn (S.-M. Hu).

https://doi.org/10.1016/j.jqsrt.2019.03.004
0022-4073/

band used to monitor nitrous oxide by the TCCON network has been studied by Werwein et al. [14,15] at 2.26 µm. The self- and air-induced line shape parameters were obtained with high accuracy for 41 lines of R branch with the maximum rotational quantum number of 40.

In this study, we present the study on the 00°3 – 00°0 band of nitrous oxide, including measurements of 88 lines at low pressures, and N_2-broadened spectral line shapes of 20 well isolated lines. Line positions were determined and the N_2-induced line broadening and shifting coefficients were derived from fit of the spectra using different line profiles.

2. Experimental details

The experimental setup is similar to the laser-locked cavity ring-down spectrometer described in Refs [16–20]. Briefly, the structure of the setup is as follows: the *s*-polarization probe laser is an external cavity diode laser (ECDL, Toptica DL Pro-1550) which is locked to a temperature-stabilized ring-down (RD) Invar cavity using the Pound-Drever-Hall (PDH) method. The RD cavity is composed of a pair of high-reflectivity (99.996% at 1.5 – 1.7 µm, Layertec GmbH Inc.) mirrors with a distance of 110.8 cm, leading to a free spectral range (FSR) of 135.27 MHz, a finesse of 78,000 and a mode width of about 1.6 kHz. The RD cavity is thermal-stabilized at 298.8 K with a fluctuation less than 50 mK. Its absolute frequency is calibrated by an optical frequency comb which is synthesized by an Er: fiber oscillator operated at 1.56 µm. The repetition frequency ($f_R \approx 180$ MHz) and carrier offset frequency (f_0) of the comb are locked to accurate radio-frequency sources, both referenced to a Global Positioning System (GPS)-discipline rubidium clock (SRS FS725). The beat signals between the probe laser and the comb were recorded by a frequency counter (Agilent 53181A).

A separated *p*-polarization probe laser beam, frequency shifted by an acousto-optic modulator (AOM) and a fiber electro-optic modulator (EOM), is coupled into the RD cavity from the other side of the cavity and used for cavity ring-down spectroscopy (CRDS) measurements. The *s*- and *p*-polarization beams were separated with a combination of polarizing waveplates and Glan-Taylor prism for frequency locking and spectral probing. The AOM serves as a beam chopper, which is triggered by an external rectangle wave to shut off the CRDS-probing beam to initial a ring-down event. The ring-down curve is fit by an exponential decay function to derive the decay time τ, and the sample absorption coefficient α is determined from the change of the cavity loss rate: $\alpha = (c\tau)^{-1} - (c\tau_0)^{-1}$, where c is the speed of light, and τ and τ_0 are decay times of the cavity with and without sample, respectively.

The Doppler-limited spectra were recorded with natural nitrous oxide sample (Nanjing ShangYuan 99.0% stated purity) at three pressures (1.0, 3.0, and 4.0 Pa) depending on the absorption intensities of the measured lines. In total, 88 lines with intensities stronger than 1×10^{-24} cm^{-1}/(molecule cm^{-2}) were studied. The N_2 gas sample with high stated purity of 99.99% (Nanjing ShangYuan) was used as the buffer gas. For the N_2-broadened spectra, the total pressures varied from 1.0 kPa to 50.0 kPa with the N_2O volume mixing ratios less than 0.1%. Sample pressures were measured by capacitance gauges, Pfeiffer Vacuum CCR 372 (full range 13.3 kPa) with a stated accuracy of 0.15%, and Shanghai Zhentai Instruments Co. CPCA-140Z (full range 100 kPa) with stated accuracy of 0.5%. The absorption spectra of each line at each experimental condition was recorded 30 times to reach enough signal-to-noise level. To avoid the interference from neighbor absorptions of other molecules and isotopologues, the N_2-broadened spectra of 20 well-isolated transitions in the 0003 – 0000 band were measured in this work. Note that the FSR of the ring-down cavity was measured for each line with high pressure samples to correct the frequency shift due to dispersion.

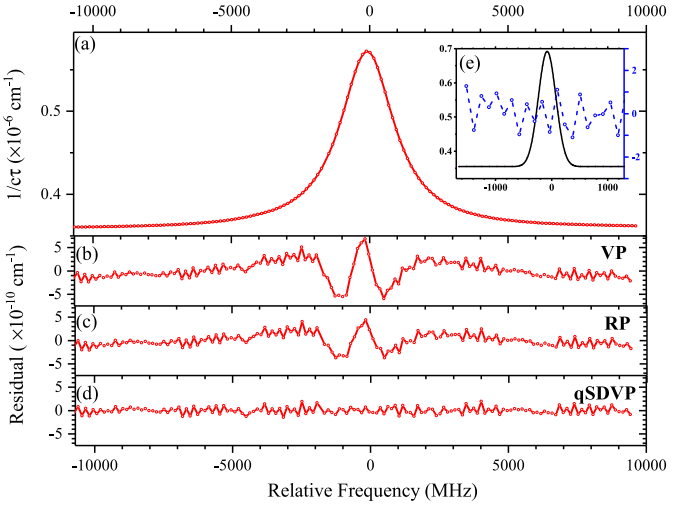

Fig. 1. Examples of CRDS-spectrum for the P(19) line recorded with sample pressures of 1 Pa (e) and 50 kPa (a), along with the residuals retrieved with Voigt profile (b), Rautian profile (c), and quadratic speed-dependent Voigt profile (d). Note that the spectra refer to the left vertical axis, while the residuals refer to the right vertical axis. A factor of 10,000 enlargement was applied in the right vertical axis in the (e) layer.

3. Line positions

3.1. Line positions determination

The Doppler-limited spectra were fitted using a least-square fitting program assuming a Voigt profile with the Gaussian width fixed to the theoretical value of the Doppler broadening. The inserted plot of Fig. 1(e) shows the spectra of P(19) line recorded with a sample pressure of 1.0 Pa together with the fitting residuals of the measured spectra, which illustrate a noise equivalent absorption coefficient at the 7.5×10^{-11} cm^{-1} level.

The self-induced shifts of studied transitions in this work have not been reported in literatures. As far as we know, the self-induced shifts have been reported for 177 lines of ten vibrational bands below 4400 cm^{-1} in Refs [12,14,21]. The average value of the self-induced shifts was found to be −0.0015(6) cm^{-1}/atm (1atm=101 325.0 Pa) encompassing all 136 transitions in nine vibrational bands below 2360 cm^{-1} by Toth [12], which differs from the value −0.00405 cm^{-1}/atm adopted by Pollock et al. [21]. While the self-induced shifts show linear depending on J values for the 0002 – 0000 band by Werwein et al. [14], which vary between −0.00228 and −0.00641 cm^{-1}/atm. The maximum absolute value of the self-induced shift is assumed not exceeding 0.01 cm^{-1}/atm, which is about 12 kHz at a pressure of 4.0 Pa. Therefore, the self-induced shifts of the line center can be neglected in our Doppler-limited spectra.

The position of P(40) is determined to be 195 800 327.99 MHz (1cm^{-1} = 29 979.2458 MHz) and the uncertainty budget is presented in Table 1. A statistical uncertainty of 0.08 MHz was obtained by averaging the results derived from 20 spectra recorded in half an hour. The frequency comb used for calibration has an uncertainty of 0.4 kHz due to the long term stability of 2×10^{-12} from the Rb clock. The frequency drift due to the thermal expansion of the cavity was smaller than 0.02 MHz in each scan according to the observation in Ref. [20]. The uncertainty in the driving frequencies of the AOM and EOM are negligible. As discussed above, an uncertainty of 0.01 MHz was given for possible contribution from the pressure shift at pressures less than 4.0 Pa. Since the amplitude of the fitting residual around peak center is at the noise level, we estimate that the shift due to the asymmetry in the line

Table 1
1-σ Uncertainty budget of the P(40) line in the $3\nu_3$ band of $^{14}N_2{}^{16}O$ (in MHz).

Source	Uncertainty	
	Type A	Type B
Statistical	0.08	
Frequency comb		<0.001
Cavity drift		0.02
EOM frequency		<0.001
AOM frequency		<0.001
Pressure shift		0.01
Line profile asymmetry		0.15
Total	0.17	

profile, if any, should be below 0.15 MHz, as the full Doppler width (~360 MHz) divided by the typical signal-to-noise ratio of 2400. The overall uncertainty (1-σ, throughout this paper) of the P(40) line position is 0.17 MHz. In total, 88 lines were measured with the maximum J'' value of 47 for the $3\nu_3$ band of $^{14}N_2{}^{16}O$. Their line positions are given in Table 2. The statistical and systematic uncertainties are also included in Table 2.

3.2. Ro-vibrational spectroscopic constants

Rotational energies of the $3\nu_3$ upper vibrational state can be given by the usual formula:

$$E(J) = G_v + B_v J(J+1) - D_v J^2(J+1)^2 + H_v J^3(J+1)^3 + \cdots \quad (1)$$

Where J is the angular momentum quantum number, G_v is the vibrational term, B_v, D_v, and H_v are rotational and centrifugal distortion constants. The ro-vibrational constants can be derived from a fit of the energies given in Table 2. The ground state constants were constrained to the values given in Ref [8]. The spectroscopic constants are determined to be 197 289 025.234(56) MHz, 12,250.59678(29) MHz, 5.24157(38) kHz, and 1.74(14) mHz for G_v, B_v, D_v, and H_v, respectively. The root-mean-square deviation is 0.25 MHz, being consistent with the line position uncertainty.

3.3. Ground state combination difference comparison

Ground state combination difference (GSCD) between the P($J+1$) and R(J-1) transitions sharing the same J upper rotational state is independent on the upper energy level. The quantity value of GSCD can be calculated with the equation: $\Delta(J) = R(J-1) - P(J+1)$. The differences between the GSCD values obtained from the saturated absorption spectroscopy by Ting et al. [8], by Al Saif et al. ($v=1$) [10], and those determined in this work are presented in Fig. 2 for a comparison. The averaged values with standard deviations (1σ) are 0.13 ± 0.34 and 0.11 ± 0.28 MHz for the differences from Ting's [8] and Al Saif's [10] values, respectively, which coincide with the line position uncertainty.

3.4. Comparison to the line positions in HITRAN

The line-by-line parameters of $3\nu_3$ band have been included in the HITRAN2004 database [22] for the first time with Toth's linelist [23]. The line positions and intensities have not been updated in HITRAN2016 [24]. The deviations from HITRAN values are plotted in Fig. 3. The differences show clear J dependence. The averaged difference with standard deviation (1σ) is 3.08 ± 1.43 MHz. The stated uncertainties are 0.001 – 0.0001 cm^{-1} (3–30 MHz) given in the HITRAN database, being consistent with the comparison given here.

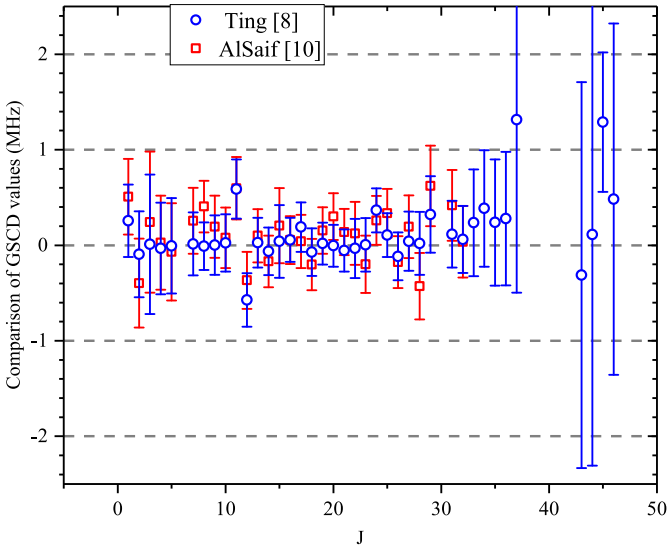

Fig. 2. Comparisons of GSCD values obtained from Ting et al. [8] and Al Saif et al. [10] and those determined in this study with the rotational quantum number J of the upper state.

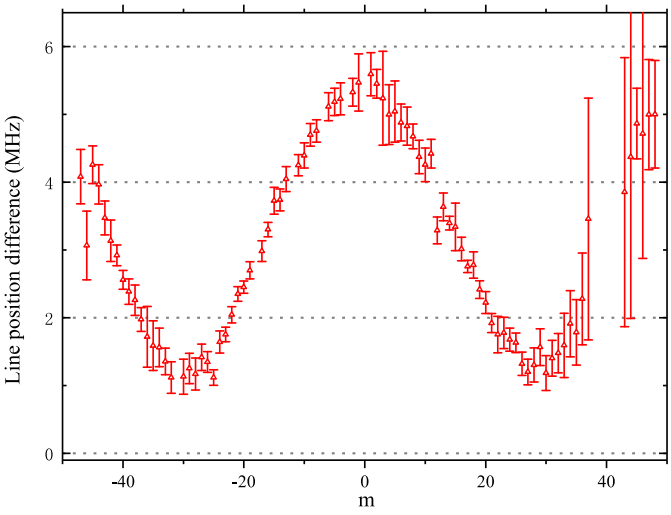

Fig. 3. Comparisons of line positions of $^{14}N_2{}^{16}O$ for 88 transitions of $3\nu_3$ band from the values in HITRAN2016 database with the quantum number m of the lower state (m is the $-J$ in the P-branch and $J+1$ in the R-branch).

4. Nitrogen-induced line shape parameters

N_2-broadened spectra were fitted with the Voigt profile, Rautian profile and the quadratic Speed-Dependent Voigt (qSDV) profile, respectively. The nonlinear spectra fitting program was written based on the line shape model proposed by Ngo et al. [25]. The line center, intensity, collision broadening width, Dicke narrowing coefficient, speed-dependent parameters and the linear polynomial parameters for baseline were derived from the least-square fit. Note that the speed-dependence for shifting parameters were set to be zero in the fit. As shown in Fig. 1(a-d), the spectra of P(19) line was recorded at 50 kPa and fitted with different line profiles. The W-shaped structure of the fitting residuals presents in the fit of the Voigt profile, especially at high pressures. If the speed-dependence was neglected, the remained residuals from the fit of Rautian profile still showed obvious deviations above the noise level while the qSDV profile could fit the experimental spectra quite well to the noise level. The pressure-induced line shape parameters of a transition corresponds to the slope of the

Table 2
Line positions of the $3\nu_3$ band of $^{14}N_2{}^{16}O$ and the derived upper level energies (in MHz). Ground state rotational constants are from Ref. [8].

J"	P(J")	Uncertainty		J"	R(J")	Uncertainty		J'	E'
		Statis.	Sys.			Statis.	Sys.		
P(1)	197,263,901.97(42)	0.12	0.40					0	197,289,025.22(42)
P(2)	197,238,156.83(21)	0.06	0.20	R(0)	197,313,526.19(32)	0.09	0.31	1	197,313,526.32(40)
P(3)	197,211,789.70(40)	0.15	0.34	R(1)	197,337,405.40(21)	0.06	0.20	2	197,362,528.60(45)
P(4)	197,184,801.07(24)	0.12	0.21	R(2)	197,360,662.02(69)	0.15	0.68	3	197,436,031.64(73)
P(5)	197,157,190.83(20)	0.10	0.18	R(3)	197,383,296.29(44)	0.11	0.43	4	197,534,035.13(48)
P(6)	197,128,959.14(21)	0.08	0.19	R(4)	197,405,307.90(45)	0.10	0.44	5	197,656,538.47(50)
P(7)				R(5)	197,426,696.76(27)	0.08	0.26	6	197,803,541.04(27)
P(8)	197,070,631.88(17)	0.07	0.15	R(6)	197,447,462.84(28)	0.07	0.27	7	197,975,042.18(33)
P(9)	197,040,536.67(17)	0.06	0.16	R(7)	197,467,606.04(18)	0.06	0.17	8	198,171,041.00(25)
P(10)	197,009,820.54(19)	0.05	0.18	R(8)	197,487,126.13(25)	0.06	0.24	9	198,391,536.43(31)
P(11)	196,978,483.68(16)	0.05	0.15	R(9)	197,506,023.07(25)	0.05	0.24	10	198,636,527.41(30)
P(12)	196,946,526.46(23)	0.12	0.20	R(10)	197,524,296.45(21)	0.05	0.21	11	198,906,012.64(43)
P(13)	196,913,948.16(19)	0.04	0.18	R(11)	197,541,947.56(20)	0.05	0.19	12	199,199,991.01(40)
P(14)	196,880,749.75(16)	0.04	0.16	R(12)	197,558,973.63(20)	0.07	0.19	13	199,518,460.12(26)
P(15)	196,846,931.08(20)	0.04	0.19	R(13)	197,575,376.71(15)	0.04	0.15	14	199,861,419.25(25)
P(16)	196,812,492.54(15)	0.04	0.15	R(14)	197,591,156.05(35)	0.05	0.35	15	200,228,866.45(38)
P(17)	196,777,433.93(15)	0.04	0.15	R(15)	197,606,311.48(17)	0.07	0.16	16	200,620,799.64(23)
P(18)	196,741,755.69(21)	0.05	0.20	R(16)	197,620,842.98(15)	0.04	0.15	17	201,037,217.00(28)
P(19)	196,705,457.34(16)	0.06	0.15	R(17)	197,634,750.33(19)	0.07	0.18	18	201,478,116.03(25)
P(20)	196,668,539.95(16)	0.04	0.15	R(18)	197,648,033.60(15)	0.05	0.15	19	201,943,495.02(22)
P(21)	196,631,003.04(15)	0.05	0.15	R(19)	197,660,692.52(16)	0.07	0.15	20	202,433,351.18(22)
P(22)	196,592,846.96(16)	0.05	0.15	R(20)	197,672,727.10(15)	0.05	0.15	21	202,947,682.15(22)
P(23)	196,554,071.79(16)	0.05	0.15	R(21)	197,684,137.07(27)	0.08	0.26	22	203,486,485.19(31)
P(24)	196,514,677.68(16)	0.05	0.16	R(22)	197,694,922.38(23)	0.05	0.22	23	204,049,757.54(28)
P(25)	196,474,665.20(16)	0.06	0.15	R(23)	197,705,083.04(17)	0.05	0.16	24	204,637,496.60(30)
P(26)	196,434,033.50(16)	0.06	0.15	R(24)	197,714,618.89(16)	0.06	0.15	25	205,249,698.81(23)
P(27)	196,392,783.49(19)	0.08	0.18	R(25)	197,723,529.93(17)	0.06	0.16	26	205,886,361.46(26)
P(28)	196,350,915.32(24)	0.07	0.23	R(26)	197,731,815.71(19)	0.06	0.18	27	206,547,481.09(31)
P(29)	196,308,428.95(22)	0.09	0.20	R(27)	197,739,476.50(25)	0.07	0.24	28	207,233,054.42(34)
P(30)	196,265,324.61(29)	0.10	0.24	R(28)	197,746,511.77(27)	0.07	0.26	29	207,943,077.73(43)
P(31)				R(29)	197,752,922.32(26)	0.08	0.25	30	208,677,547.80(26)
P(32)	196,177,262.69(23)	0.12	0.20	R(30)	197,758,707.19(26)	0.09	0.25	31	209,436,460.53(36)
P(33)	196,132,305.27(20)	0.13	0.15	R(31)	197,763,866.54(29)	0.10	0.27	32	210,219,811.96(36)
P(34)	196,086,730.62(29)	0.14	0.25	R(32)	197,768,400.19(48)	0.11	0.46	33	211,027,598.20(58)
P(35)	196,040,538.87(37)	0.16	0.33	R(33)	197,772,308.27(49)	0.12	0.47	34	211,859,815.19(65)
P(36)	195,993,730.04(45)	0.17	0.41	R(34)	197,775,590.82(48)	0.13	0.46	35	212,716,458.64(67)
P(37)	195,946,304.12(17)	0.05	0.17	R(35)	197,778,247.09(68)	0.15	0.66	36	213,597,523.74(72)
P(38)	195,898,261.79(23)	0.06	0.22	R(36)	197,780,276.7(18)	0.2	1.8	37	214,503,006.1(19)
P(39)	195,849,602.95(19)	0.07	0.17	R(37)	-			38	215,432,902.40(22)
P(40)	195,800,327.99(17)	0.08	0.15	R(38)	-			39	216,387,206.32(20)
P(41)	195,750,436.47(17)	0.07	0.15	R(39)	-			40	217,365,912.99(21)
P(42)	195,699,929.32(32)	0.28	0.15	R(40)	-			41	218,369,018.14(35)
P(43)	195,648,806.27(25)	0.12	0.22	R(41)	-			42	219,396,516.17(30)
P(44)	195,597,067.60(29)	0.14	0.25	R(42)	197,779,313.4(20)	0.4	1.9	43	220,448,402.1(20)
P(45)	195,544,713.65(28)	0.12	0.25	R(43)	197,776,960.1(24)	0.4	2.3	44	221,524,670.1(24)
P(46)	195,491,745.71(51)	0.21	0.46	R(44)	197,773,980.77(52)	0.15	0.50	45	222,625,315.7(10)
P(47)	195,438,160.69(40)	0.23	0.33	R(45)	197,770,374.8(18)	0.6	1.7	46	223,750,331.5(19)
				R(46)	197,766,142.35(81)	0.21	0.79	47	224,899,713.01(84)
				R(47)	197,761,283.31(79)	0.25	0.76	48	226,073,454.37(83)

respective linear regressions. Fig. 4 shows the Lorentzian widths (upper panel) and the line centers (lower panel) with respect to the total pressures for R(7) (dot line) and P(19) (dash line) transitions. It is clear that the broadening coefficients retrieved from the qSDV profile (blue) are about 3.5% larger than the values from the Voigt profile (red). The fitted lines with line shape parameters cross the zero point. The self-induced components are negligible since the nitrous oxide volume mixing ratios are less than 0.1%. Table 3 summarized the retrieved N_2-broadening and shift parameters by Voigt profile and qSDV profile, as well as the speed-dependence parameter γ_2 from linear fit of Γ_0, Δ_0 and Γ_2 resulting from line shape models on pressure. Due to the experimental limitation, we did not observe pressure induced shift parameters for transitions P(7) and P(31). These parameters were all given at 298.8 K which is the stabilized temperature of the ring-down cavity. The uncertainty of the line shape parameters retrieved in this work results from both temperature and pressure. The pressure gauges were calibrated at National Institute of Metrology, China. The absolute relative uncertainties at different pressure series are 0.25% (<13.3 kPa) and 0.5% (>13.3 kPa). The temperature uncertainty of the ring-down cavity was estimated to be 0.05 K at maximum. For the temperature dependence of the line shape parameters modeled by the power law $X(T, P) = P \cdot X(T_{ref}) \cdot (T_{ref}/T)^n$, the assumed scaling factor for temperature dependence would be 99.3% for $n = 0.75$ compared to the reference temperature 296 K. Therefore, the total errors given in Table 3 were calculated as a sum of the described uncertainties from experimental error sources and the statistical errors from the fitting procedure.

The pressure broadening and shift coefficients were fitted using a third-order polynomial function:

$$X(m) = a_0 + a_1|m| + a_2|m|^2 + a_3|m|^3, 2 \leq m \leq 45$$

X represents for γ_0 (N_2-induced broadening coefficient) and δ_0 (N_2-induced shift coefficient) with $m = -J$ and $m = J+1$ for the P and R branch, respectively. Note that the broadening parameters for N_2O would only be extrapolated for m up to 45. As shown in

Table 3
N_2-broadening and shift parameters with 1-σ uncertainty for the 00°3 – 00°0 band of $^{14}N_2{}^{16}O$ at 1.54 μm at temperature 298.8 K.

Line	γ_0 (cm^{-1}/atm)		γ_2 (cm^{-1}/atm)	δ_0 (cm^{-1}/atm)	
	VP	qSDVP	qSDVP	VP	qSDVP
P(45)	0.07010(77)	0.07281(43)	0.00632(33)	−0.006900(56)	−0.007034(38)
P(41)	0.07045(70)	0.07318(38)	0.00602(12)	−0.006811(42)	−0.006965(41)
P(31)	0.07185(48)	0.07494(39)	0.00677(21)	–	–
P(28)	0.07191(70)	0.07576(43)	0.00704(13)	−0.00650 (10)	−0.00651 (12)
P(22)	0.07593(89)	0.07804(41)	0.00749(14)	−0.006353(41)	−0.006405(97)
P(19)	0.07755(93)	0.07980(41)	0.00800(17)	−0.006098(34)	−0.00624 (11)
P(18)	0.07780(61)	0.08028(41)	0.00808(16)	−0.006079(40)	−0.006273(47)
P(12)	0.08242(66)	0.08526(47)	0.00874(19)	−0.005637(40)	−0.005734(66)
P(9)	0.0854(10)	0.08811(45)	0.00879(19)	−0.005387(62)	−0.00565 (13)
P(7)	0.08733(65)	0.09018(47)	0.00910(21)	–	–
P(3)	0.09354(78)	0.09582(62)	0.00957(60)	−0.00424 (14)	−0.00439 (14)
R(0)	0.0995 (10)	0.10277(73)	0.01067(71)	−0.003037(79)	−0.00289 (14)
R(3)	0.08908(99)	0.09345(58)	0.00909(49)	−0.003932(88)	−0.00394 (12)
R(5)	0.0889(11)	0.09121(52)	0.00889(24)	−0.004194(36)	−0.00432 (13)
R(7)	0.0865(11)	0.08907(53)	0.00898(34)	−0.004408(32)	−0.004537(94)
R(12)	0.0815(10)	0.08426(48)	0.00871(19)	−0.004953(29)	−0.005003(37)
R(15)	0.07904(97)	0.08164(43)	0.00849(09)	−0.005266(36)	−0.005357(49)
R(17)	0.07556(74)	0.07989(43)	0.00813(14)	−0.005536(51)	−0.005607(62)
R(19)	0.07647(88)	0.07883(42)	0.00787(12)	−0.005785(39)	−0.005938(56)
R(21)	0.07561(89)	0.07782(41)	0.00773(18)	−0.005998(40)	−0.006064(68)

Table 4
Parameters for the polynomial function in Eq. (2) used to fit N_2-broadening and shift parameters retrieved by different line shape models as functions of m.

	γ_0 (cm^{-1}/atm) for P and R branch			δ_0 (cm^{-1}/atm) for P branch		δ_0 (cm^{-1}/atm) for R branch	
	HITRAN [22]	This work (VP)	This work(qSDVP)	This work (VP)	This work (qSDVP)	This work (VP)	This work (qSDVP)
a_0	0.0964	0.09697(95)	0.10002(60)	$-3.90(21)\times10^{-3}$	$-3.92(22)\times10^{-3}$	$-2.86(14)\times10^{-3}$	$-2.75(25)\times10^{-3}$
a_1	-1.72×10^{-3}	$-1.56(17)\times10^{-3}$	$-1.63(11)\times10^{-3}$	$-1.98(32)\times10^{-4}$	$-2.14(31)\times10^{-4}$	$-2.87(40)\times10^{-4}$	$-3.22(79)\times10^{-4}$
a_2	3.81×10^{-5}	$3.01(84)\times10^{-5}$	$3.44(53)\times10^{-5}$	$5.1(15)\times10^{-6}$	$5.7(14)\times10^{-6}$	$1.39(35)\times10^{-5}$	$1.64(72)\times10^{-5}$
a_3	-2.96×10^{-7}	$-1.9(12)\times10^{-7}$	$-2.56(74)\times10^{-7}$	$-4.9(21)\times10^{-8}$	$-5.5(19)\times10^{-8}$	$-3.40(93)\times10^{-7}$	$-4.0(19)\times10^{-7}$

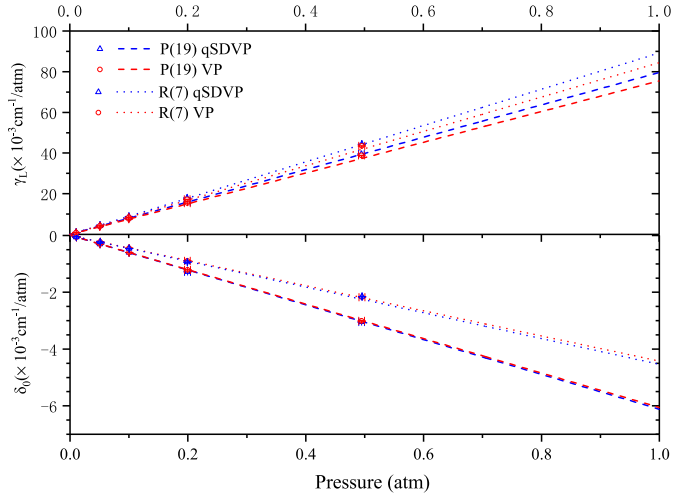

Fig. 4. Linear regressions of the Lorentzian widths (upper panel) and the line centers (lower panel) with respect to the total pressures for R(7) (dot line) and P(19) (dash line) transitions. The line shape parameters retrieved with the qSDVP profile and Voigt profile (VP) are shown in blue and red color, respectively. For the purpose of a better illustration, the respective Doppler limited line positions of nitrous oxide were subtracted from the fitted line positions. (For interpretation of the references to color in this figure legend, the reader is referred to the web version of this article.)

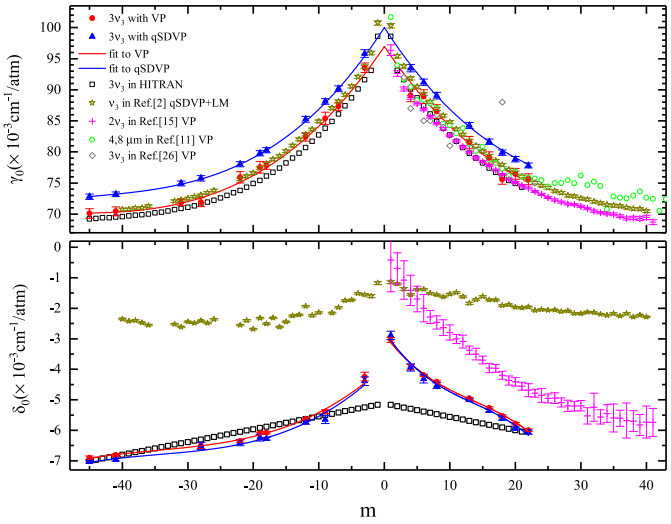

Fig. 5. The pressure broadening and shift parameters retrieved in this work from two different line shape models were plotted on the upper and lower panels, as well as the air-broadening and shift parameters taken from HITRAN database (black square), Ref. [2] (fitted from qSDVP with line-mixing, brown star), Ref. [15] (fitted from VP, pink cross), the N_2-broadening parameters from Ref. [11] (fitted from VP, green open circle) and Ref. [26] (fitted from VP, open diamond); and a third-order polynomial function were used to fit as functions of *m*.

Fig. 5, the pressure broadening and shift parameters retrieved in this work from two different line shape models were plotted in the upper and lower panels and fitted to Eq. 2 as a function of *m*. Table 4 summarized the *m*-dependence parameters for N_2-broadening and shift coefficients which were fitted using the third-order polynomial function described above. The P and R branch polynomials for the N_2-broadening coefficients were constrained to have the same values because the m-dependence for the P and R branches shows a symmetric pattern. For the region around *m* equal to zero, the polynomial fit did not represent well. The

comparison between γ_0 retrieved in this work from both Voigt and qSDV profile shows in Fig. 5, and in general, the γ_0 retrieved from qSDVP were slightly larger than that from Voigt profile. Furthermore, the γ_{air} value taken from HITRAN database [24] as well as the air-broadening γ_0 value retrieved from qSDVP with line-mixing for the ν_3 band in Ref. [2] and that for the $2\nu_3$ band in Ref. [15] shows good agreement with slight difference contributed from the O_2-broadening proportion and temperature dependence different from the reference temperature at 296 K. The N_2-broadening parameters taken from Refs. [11,26] retrieved with Voigt profile were also shown in Fig. 5, which are about 1–2% different from our measurements within the experimental uncertainties. As for the pressure-induced line shift vs. the m quantum number shown on the lower panel of Fig. 5, a clear asymmetry in the m-dependence for P and R branches was presented. Therefore, separated polynomial fit was performed according to Eq. 2, for the P and R branches, respectively. The same comparison between this work and the HITRAN database [24] shows clear deviations in both P and R branches. And the comparisons to the transitions of the ν_3 and $2\nu_3$ bands of pressure-induced shift parameters present some tendency on vibrational quantum number.

5. Conclusion

We present the absorption spectroscopic analysis of the 00°3 – 00°0 band of $^{14}N_2{}^{16}O$ near 1.54 μm recorded by a laser-locked cavity ring-down spectrometer referenced to an optical frequency comb. Doppler limited line positions were determined with sub-MHz uncertainty for 88 transitions. N_2-induced broadening and shift coefficients were obtained with a relative uncertainty of about 1% for 20 isolated transitions by using the Voigt and qSDV profile models. Deviations of 1–5 MHz were found between the line positions determined in this work and those given in the HITRAN line list based on FTS measurements by Toth [23]. The N_2-induced broadening coefficients for the $3\nu_3$ band obtained in the present study are in good agreement with most of the literature values listed above for other bands [2,11,15,26].

Acknowledgment

This work is jointly supported by the NSFC (21473172, 21427804 and 21688102), NBRPC (No. 2013CB834602), and CAS (No. XDB21020100).

Supplementary materials

Supplementary material associated with this article can be found, in the online version, at doi:10.1016/j.jqsrt.2019.03.004.

References

[1] Ravishankara AR. Nitrous Oxide: the Dominant Ozone-Depleting Substance Emitted in the 21st Century. Science 2009;326:123–5. doi:10.1126/science.1176985.
[2] Loos J, Birk M, Wagner G. Pressure broadening, -shift, speed dependence and line mixing in the ν_3 rovibrational band of N_2O. J Quant Spectrosc Radiat Transf 2015;151:300–9. doi:10.1016/j.jqsrt.2014.10.008.
[3] United Nations Environment Programme. Intergovernmental Panel on Climate Change, Fourth Assessment Report. 2007. https://www.ipcc.ch/.
[4] Wunch D, Toon GC, Blavier JFL, Washenfelder RA, Notholt J, Connor BJ, et al. The total carbon column observing network. Philos Trans R Soc A Math Phys Eng Sci 2011;369:2087–112. doi:10.1098/rsta.2010.0240.
[5] Toon G, Blavier J-F, Washenfelder R, Wunch D, Keppel-Aleks G, Wennberg P, et al. Total Column Carbon Observing Network (TCCON). Adv Imag 2009 JMA3. doi:10.1364/FTS.2009.JMA3.
[6] Schneider M, Hase F, Blavier JF, Toon GC, Leblanc T. An empirical study on the importance of a speed-dependent Voigt line shape model for tropospheric water vapor profile remote sensing. J Quant Spectrosc Radiat Transf 2011;112:465–74. doi:10.1016/j.jqsrt.2010.09.008.
[7] Tran H, Rohart F, Boone C, Eremenko M, Hase F, Bernath P, et al. Non-Voigt line-shape effects on retrievals of atmospheric ozone: collisionally isolated lines. J Quant Spectrosc Radiat Transf 2010;111:2012–20. doi:10.1016/j.jqsrt.2010.04.002.
[8] Ting W-J, Chang C-H, Chen S-E, Chen H-C, Shy J-T, Drouin BJ, et al. Precision frequency measurement of N_2O transitions near 45 μm and above 150 μm. J Opt. Soc. Am. B 2014;31:1954. doi:10.1364/JOSAB.31.001954.
[9] Chen T-L, Liu Y-W. Sub-Doppler resolution near-infrared spectroscopy at 128 μm with the noise-immune cavity-enhanced optical heterodyne molecular spectroscopy method. Opt. Lett. 2017;42:2447. doi:10.1364/OL.42.002447.
[10] AlSaif B, Lamperti M, Gatti D, Laporta P, Fermann M, Farooq A, et al. High accuracy line positions of the ν_1 fundamental band of $^{14}N_2{}^{16}O$. J. Quant. Spectrosc. Radiat. Transf. 2018;211:172–8. doi:10.1016/j.jqsrt.2018.03.005.
[11] Lacome N, Levy A, Guelachvili G. Fourier transform measurement of self-, N_2-, and O_2-broadening of N_2O lines: temperature dependence of linewidths. Appl. Opt. 1984;23:425. doi:10.1364/AO.23.000425.
[12] Toth RA. Line strengths (900 – 3600 cm^{-1}), self-broadened linewidths, and frequency shifts (1800 – 2360 cm^{-1}) of N_2O. Appl. Opt. 1993;32:7326. doi:10.1364/AO.32.007326.
[13] Vitcu A, Ciurylo R, Wehr R, Drummond JR, May AD. Broadening, shifting, and line mixing in the 0310 ← 0110 parallel Q branch of N_2O. J. Mol. Spectrosc. 2004;226:71–80. doi:10.1016/j.jms.2004.03.017.
[14] Werwein V, Brunzendorf J, Serdyukov A, Werhahn O, Ebert V. First measurements of nitrous oxide self-broadening and self-shift coefficients in the 0002-0000 band at 2.26 μm using high resolution Fourier transform spectroscopy. J. Mol. Spectrosc. 2016;323:28–42. doi:10.1016/j.jms.2016.01.010.
[15] Werwein V, Li G, Serdyukov A, Brunzendorf J, Werhahn O, Ebert V. High-resolution Fourier transform measurements of air-induced broadening and shift coefficients in the 0002–0000 main isotopologue band of nitrous oxide. J. Mol. Spectrosc. 2018;348:68–78. doi:10.1016/j.jms.2017.07.002.
[16] Wang J, Sun YR, Tao LG, Liu AW, Hua TP, Meng F, et al. Comb-locked cavity ring-down saturation spectroscopy. Rev. Sci. Instrum. 2017;88. doi:10.1063/1.4980037.
[17] Tao LG, Liu AW, Pachucki K, Komasa J, Sun YR, Wang J, et al. Toward a determination of the proton-electron mass ratio from the lamb-dip measurement of HD. Phys Rev Lett 2018;120:1–5. doi:10.1103/PhysRevLett.120.153001.
[18] Wang J, Sun YR, Tao LG, Liu AW, Hu SM. Communication: molecular near-infrared transitions determined with sub-kHz accuracy. J Chem Phys 2017;147:091103. doi:10.1063/1.4998763.
[19] Tao LG, Hua TP, Sun YR, Wang J, Liu AW, Hu SM. Frequency metrology of the acetylene lines near 789 nm from lamb-dip measurements. J Quant Spectrosc Radiat Transf 2018;210:111–15. doi:10.1016/j.jqsrt.2018.02.021.
[20] Kang P, Wang J, Liu GL, Sun YR, Zhou ZY, Liu AW, et al. Line intensities of the 30011e – 00001e band of $^{12}C^{16}O_2$ by laser-locked cavity ring-down spectroscopy. J Quant Spectrosc Radiat Transf 2018;207:1–7. doi:10.1016/j.jqsrt.2017.12.013.
[21] Pollock CR, Petersen FR, Jennings DA, Wells JS, Maki AG. Absolute frequency measurements of the 0002-0000, 2001-0000, and 1201-0000 bands of N_2O by heterodyne spectroscopy. J Mol Spectrosc 1984;107:62–71. doi:10.1016/0022-2852(84)90265-0.
[22] Rothman LS, Jacquemart D, Barbe A, Chris Benner D, Birk M, Brown LR, et al. The HITRAN 2004 molecular spectroscopic database. J Quant Spectrosc Radiat Transf 2005;96:139–204. doi:10.1016/j.jqsrt.2004.10.008.
[23] Toth RA. "Linelist of N2O parameters from 500 to 7500 cm^{-1}", database. http://mark4sun.jpl.nasa.gov/n2o.html.
[24] Gordon IE, Rothman LS, Hill C, Kochanov RV, Tan Y, Bernath PF, et al. The HITRAN2016 molecular spectroscopic database. J Quant Spectrosc Radiat Transf 2017;203:3–69. doi:10.1016/j.jqsrt.2017.06.038.
[25] Ngo NH, Lisak D, Tran H, Hartmann JM. An isolated line-shape model to go beyond the Voigt profile in spectroscopic databases and radiative transfer codes. J Quant Spectrosc Radiat Transf 2013;129:89–100. doi:10.1016/j.jqsrt.2013.05.034.
[26] Nakayama T, Fukuda H, Sugita A, Hashimoto S, Kawasaki M, Aloisio S, et al. Buffer-gas pressure broadening for the (0003) ← (0000) band of N_2O measured with continuous-wave cavity ring-down spectroscopy. Chem Phys 2007;334:196–203. doi:10.1016/j.chemphys.2007.03.001.